Am J Physiol Renal Physiol 292: F1501–F1512, 2007.
First published February 6, 2007; doi:10.1152/ajprenal.00487.2005.

NHE8 mediates amiloride-sensitive Na^+/H^+ exchange across mosquito Malpighian tubules and catalyzes Na^+ and K^+ transport in reconstituted proteoliposomes

Wanyoike Kang'ethe,[1] Karlygash G. Aimanova,[2] Ashok K. Pullikuth, and Sarjeet S. Gill[1,2]

[1]*Graduate Program in Environmental Toxicology,* [2]*Department of Cell Biology and Neuroscience, University of California, Riverside, California*

Submitted 7 December 2005; accepted in final form 26 January 2007

Kang'ethe W, Aimanova KG, Pullikuth AK, Gill SS. NHE8 mediates amiloride-sensitive Na^+/H^+ exchange across mosquito Malpighian tubules and catalyzes Na^+ and K^+ transport in reconstituted proteoliposomes. *Am J Physiol Renal Physiol* 292: F1501–F1512, 2007. First published February 6, 2007; doi:10.1152/ajprenal.00487.2005.—Following a blood meal, the mosquito *Aedes aegypti* will have acquired an enormous sodium load that must be rapidly excreted to restore ion homeostasis. It is a process that demands robust sodium and fluid transport capabilities. Even though the identities of the components involved in this ion transport across the mosquito Malpighian tubule epithelia have not been completely determined, electrophysiological studies suggest the contribution of a Na^+/H^+ exchanger extruding cations into the lumen driven secondarily by the proton gradient created by the V-type H^+-ATPase in the tubules' apical membrane. We have identified the putative exchanger and designated it *Ae*NHE8. Immunolocalization studies demonstrated that *Ae*NHE8 is expressed in the apical membranes of Malpighian tubules, gastric caecae, and rectum. When heterologously expressed in salt-sensitive yeast cells lacking Na^+ extrusion and Na^+/H^+ exchange proteins, *Ae*NHE8 rescues the salt-sensitive phenotype and restores the cells' ability to grow in high NaCl media. Furthermore, heterologous expression of *Ae*NHE8 in NHE-deficient fibroblast cells results in an amiloride-sensitive $^{22}Na^+$ uptake. To determine the exchanger's kinetic properties, we reconstituted membranes from yeast cells expressing the protein into lipid proteoliposomes and assayed for cation-dependent H^+ exchange by fluorimetric methods. Our results indicate that *Ae*NHE8 mediates saturable exchange of Na^+ and K^+ for H^+. We propose that *Ae*NHE8 may be coupled to the inward H^+ gradient across the Malpighian tubules and plays a role in the extrusion of excess sodium and potassium while maintaining steady intracellular pH in the principal cells.

ion homeostasis; *Aedes aegypti*; apical membrane

HEMATOPHAGOUS INSECTS SUCH as female mosquitoes require blood for oogenesis, an adapatation that facilitates the spread of such human diseases as malaria and yellow fever (9). After engorgement, the insects must rid themselves of the high sodium chloride and water load from blood plasma and potassium gained from blood cells to restore electrolytic balance in the hemolymph (35). The diuresis is initiated rapidly while the insect is still blood feeding (4) but neither the process nor its regulation is yet adequately understood at the molecular level.

It has been postulated that the feeding activates as yet unidentified mechanoreceptor(s) in the gut, which in turn prompt the release of neurosecretory factors from the brain that activate signaling pathways that regulate expression and/or activity of ion and fluid transporters in the epithelial tissue of the midgut, gastric caecae, Malpighian tubules (analogous to vertebrate kidneys), hindgut, and rectum (10, 24). Since insect Malpighian tubules are not innervated, regulation of their function is via intrinsic mechanisms and humoral messengers circulating in the hemolymph (4). One factor whose activity has been shown to increase in the mosquito's hemolymph after a blood meal is the CRF-like mosquito natriuretic peptide (MNP) (36, 56). MNP activates receptors in the Malpighian tubules, triggering the release of cAMP, which then activates Na^+ channels and Na^+-K^+-$2Cl^-$ cotransporters in the basolateral membrane of principal cells (36). Basolateral entry of Na^+ and K^+ into the principal cell also involves the mostly basolaterally localized *Ae*NHE3 (22, 40). The basolateral Na^+-K^+-ATPase likely contributes in loading K^+ into the principal cells (22, 31, 34, 51). Once the concentration of cytoplasmic Na^+ has been elevated, its competitiveness for extrusion across the apical membrane likewise increases.

In animals, the basolateral Na^+-K^+-ATPase predominantly energizes transepithelial transport; but in an appreciable number of cases, this role is played by the V-type H^+-ATPase (20, 57). In mosquitoes for instance, transport across the Malpighian tubule's principal cells is dependent on the electrochemical gradient created by the apical V-ATPase (5). ATP is generated in the dense mitochondrion present in the apical brush-border microvillus of principal cells (3, 55) and used to drive proton extrusion into the lumen. But interestingly, the luminal pH in *Aedes aegypti's* Malpighian tubules remains stable within the neutral range under both control and active diuretic conditions (37) implying that the protons extruded do not accumulate. This could arise if these protons were recycled back into the principal cells in exchange for Na^+ and/or K^+ via an apical membrane Na^+/H^+ exchanger (NHE) protein.

NHEs (solute carrier family 9, SLC 9) are members of the monovalent cation proton antiporter (CPA) superfamily of transporters that are conserved in bacteria and eukaryotes (6). By exchanging H^+ for Na^+ or K^+, they regulate cellular and systemic pH in addition to ionic concentrations in cells (21, 33). The proposed contribution of insect NHEs in epithelial ion transport has been largely inferred from electrophysiological assays involving pharmacological inhibition or activation of fluid and ion secretion in isolated Malpighian tubules (e.g.,

Address for reprint requests and other correspondence: A. K. Pullikuth, Dept. of Pharmacology and Experimental Therapeutics, Louisiana State Univ. Health Sciences Centre, New Orleans, LA 70112 (e-mail: apulli@lsuhsc.edu) and S. S. Gill, Dept. of Cell Biology and Neuroscience, Univ. of California, Riverside, CA 92521 (e-mail: sarjeet.gill@ucr.edu).

The costs of publication of this article were defrayed in part by the payment of page charges. The article must therefore be hereby marked "*advertisement*" in accordance with 18 U.S.C. Section 1734 solely to indicate this fact.

Ramsay assays) and measurement of the associated changes in pH and electric potential (5, 22, 37, 55). Recent findings that *Ae*NHE3 is predominantly expressed in the basolateral membrane of the principal cells render it an unlikely candidate for the apical exchanger (40).

In this report, we present the functional characterization of a Na^+/H^+ antiporter from the mosquito *A. aegypti*, hereafter, *Ae*NHE8. Ion transport, heterologous expression, complementation, and immunolocalization studies indicate that NHE8 is an amiloride-sensitive Na^+/H^+ antiporter located on the apical membrane of principal cells. Our data suggest that *Ae*NHE8 may play some role in the restoration of Na^+ and K^+ homeostasis in the mosquito during postblood meal diuresis.

EXPERIMENTAL PROCEDURES

Mosquitoes. Aedes aegypti larvae were fed a 3:1 mix of dog food and brewers yeast; adults were fed 3% sucrose solution in water. The mosquitoes were maintained at 26°C, 80% relative humidity with a 12:12-h light-dark photoperiod schedule. Adult females (4–10 days old) were cold-anesthetized and dissected in phosphate-buffered saline. Tissues for protein and RNA extraction were frozen in dry ice and stored at −80°C until used.

Cloning of exchanger, sequence analysis, and expression constructs. Conserved mammalian NHE signature sequences from NHE1–6 were used to identify genomic, full-length cDNA and EST exchanger sequences from *Drosophila* and *Anopheles* databases. Positive hits were classified on the basis of whether they contained or lacked the "VFFLFLLPPII" residue pocket (typically located in the 3rd or 4th transmembrane domain) that is critical for amiloride sensitivity (reviewed in Ref. 8). Putative *Anopheles* NHE8 and *Drosophila* NHE1 (16, 41) emerged as potential amiloride-sensitive exchangers. Degenerate primers were then designed against their conserved transmembrane domains to amplify candidates from an *A. aegypti* cDNA library. Identification of candidate clones was done following the Limited Growth PCR procedure as described (48). These clones were sequenced at the ends using vector primers and aligned against *Drosophila* and *Anopheles* NHE genes to ascertain their identity and completeness. A 2,864-bp-long transcript coding for the *A. aegypti* homolog of *Drosophila* NHE1 (16) and mouse NHE8 (accession no. AF482993) was identified and deposited in the NCBI GenBank database (accession no. AY326255). It differs from the sequence deposited by TIGR & Broad Institute (http://aaegypti.vectorbase.org/index.php) by one substitution, (i.e., nucleotide A457G). For comparative purposes, we performed a multiple alignment of *Ae*NHE8 sequences against known homologs (from the NCBI database) using ClustalX (50), and the output was visualized on the Boxshade 3.21 interface.

To heterologously express *Ae*NHE8, the transcript's protein coding sequence was amplified by PCR and cloned into pYES 2.1 TOPO (Invitrogen, Carlsbad, CA), a galactose-inducible yeast expression vector. To allow efficient immunoprecipitation of heterologously expressed exchanger, a c-Myc tag was added to the COOH-terminal of *Ae*NHE8 by PCR. For expression in mammalian PS120 cells, *Ae*NHE8 and *Ae*NHE8::cMyc were cloned into the pcDNA3.1(+) vector (Invitrogen). All constructs were fully sequenced to confirm that there were no PCR errors.

Expression of Aedes aegypti NHE8 in Saccharomyces cerevisiae. S. cerevisiae strains G19 (*MATα, ade2, his3, leu2, trp1, ura3,·ena1::HIS3::ena4*) and AXT3 (*MATα, ade2, his3, leu2, trp1, ura3,·ena1::HIS3::ena4, nha1::LEU2, nhx1::TRP1*) were gifts from Dr. J. M. Pardo (Consejo Superior de Investigaciones Cientificas, Sevilla, Spain) and have been previously characterized (26, 42). Yeast cells were transformed with pYES2.1 TOPO::*Ae*NHE8 by the LiCl method. Growth in high Na^+ was assayed in alkali cation-free arginine phosphate (AP) medium (46) supplemented with the appropriate concentrations of NaCl. Tolerance to hygromycin B (100 μg/ml) was assayed in minimal media.

Expression of AeNHE8 in NHE-deficient PS120 cells. NHE-deficient PS120 cells (38) were maintained in DMEM supplemented with penicillin/streptomycin (Invitrogen) and 10% fetal bovine serum (Invitrogen). To create stable PS120 cell lines expressing *Ae*NHE8 and *Ae*NHE8::c-Myc, *Mfe1* linearized constructs were transfected into the cells using Lipofectamine 2000 (Invitrogen). Selection medium (DMEM, 10% fetal bovine serum and antibiotics supplemented with 1 mg/ml G418) was added 2 days posttransfection. Growth was maintained until individual foci were apparent. Surviving cells were trypsinized and grown in selection media as individual stably transfected clones. Following confocal microscopy to determine expression, the clones showing highest expression were selected for $^{22}Na^+$ uptake assays.

Anti-NHE8 antibodies. Two hydrophilic peptides (WK-215 and WK-69) were designed based on TopPred topology and antigenicity prediction index (http://bioweb.pasteur.fr/seqanal/interfaces/toppred.html). The synthetic peptides WK-215 (C-SGGKKSRKSIRSSRL) comprising residues 511–525 and WK-69 (C-QELHDCKSQMADLTNKWYQAIRISPDDLDEEDEEDED) comprising residues 589–625 were commercially synthesized, confirmed by mass spectral analyses (Synthetic Biomolecules, San Diego, CA), and conjugated to a maleimide-activated KLH carrier protein (Pierce, Rockford, IL) via the cysteine introduced at the NH_2-terminal according to the manufacturer's protocol. This conjugate was used to immunize rabbits. Serum from subsequent bleeds was used in immunohistochemistry and immunoblotting. Antibody preadsorbed with antigen and preimmune serum were used for negative control labeling.

Immunolocalization. Fourth instar larvae and 4- to 10-day-old nonblood fed *Ae. aegypti* females were fixed overnight in 4% paraformaldehyde (PFA) at 4°C. After fixation, tissues were washed in PBS and dehydrated in a series of ethanol solutions (20, 40, 70, 95%) and finally in 100% ethanol at 4°C overnight. Samples were then passed through an ethanol/xylene series (70/30; 30/70) for 3 h each and three times in 100% xylene for 14–16 h each at room temperature (RT). Paraplast chips (Xtra, Fisher Scientific) were added to the xylene and the latter replaced with fresh Paraplast at 58°C over 2 days until tissues were completely infiltrated. These were cut into 8-μm-thick sections, and then placed on poly-L-lysine (Sigma, St. Louis, MO) and gelatin (BD, Franklin Lakes, NJ) slides and dried for 24 h at 40°C. The sections were dewaxed in 100% xylene and rehydrated in a decreasing ethanol series. They were then washed in PBS-0.1% Triton X-100 (PBST); and blocked with 2% BSA in PBST at RT. Overnight incubation followed (at 4°C) with polyclonal anti-*Ae*NHE8 antibody (WK-215 or WK-69) diluted 1:500 in 1% BSA/PBST. Washing was done with PBST containing 2% goat serum (Sigma) and 0.1% BSA. Secondary antibodies (Jackson Immunoresearch Labs, West Grove, PA): Cy3-conjugated goat-anti-rabbit IgG (for NHE8 detection,1:1,000 dilution) and Phalloidin-Alexa488 (for Actin F detection, diluted 1:100). Both were diluted in 0.1% BSA/2% goat serum/PBST; incubation was carried out in the dark at RT for 1 h. Tissues were again washed and mounted in Shur/Mount media (Electron Microscopy Sciences, Hatfield, PA). Images were obtained using a Zeiss Axioplan laser-scanning confocal microscope (LSM 510; Institute of Integrative Genome Biology, University of California, Riverside) at ×10, 40, and 100 magnification. All images were imported into Adobe PhotoShop (Version 7.0) for assembly and annotation.

A similar procedure was followed in localizing *Ae*NHE8 expressed in PS120 cells. Briefly, stable cell lines expressing untagged *Ae*NHE8 or c-Myc tagged *Ae*NHE8 were grown on single-chamber Labtek glass slides (Nunc, Rochester, NY). Cells were fixed, permeabilized, and incubated with polyclonal anti-*Ae*NHE8 (WK-69) or monoclonal anti-Myc (9E10, Santa Cruz Biotechnology) antibodies at 1:100 and 1:800 dilution, respectively. The cells were washed and stained with secondary antibodies: Cy3-conjugated goat-anti-rabbit IgG or Cy3-

conjugated goat-anti-mouse IgG, respectively (both at 1:1,000 dilution), and Alexa-488 (for Actin F detection, diluted 1:100). Images were acquired using a confocal fluorescence microscope.

Yeast cell lysis and membrane fraction recovery. Yeast AXT3 cells expressing *Ae*NHE8 and control cells transformed with a recircularized pYES2.1 vector were cultured in 2% glucose minimal medium. Cells were harvested and inoculated into galactose media (to an initial OD_{600} of 1) for induced protein expression. All batches were harvested after 20-h growth at 30°C and lysed using glass beads in lysis buffer (50 mM KH_2PO_4, pH 7.4, 500 mM NaCl, 20% glycerol) supplemented with complete inhibitor cocktail (Roche GmbH), 0.2 mM PMSF, 1 μg/ml pepstatin, and 50 mM NaF (all Sigma). Glass beads were removed by filtration and the lysate was centrifuged at 4,000 *g* to remove cell debris, the supernatant was then centrifuged at 14,600 *g* to remove mitochondria, and again further centrifuged at 200,000 *g* for 90 min. The pellets were resuspended in liposome reconstitution buffer [20 mM BTP/MES, pH 7.5, 10% glycerol, 25mM $(NH_4)_2SO_4$] at a concentration of 8 mg/ml [as determined by the BCA assay (Pierce) with BSA standards] and stored immediately at −80°C. These membrane fractions were used in vesicle reconstitution and immunoblotting.

Immunoprecipitation. PS120 cells expressing untagged *Ae*NHE8 and c-Myc-tagged *Ae*NHE8 were lysed at 2×10^7 cells/ml lysis buffer [50 mM Tris·HCl, pH 7.4, 300 mM NaCl, 5 mM EDTA, and 1% (wt/vol) Triton X-100] supplemented with protease inhibitor cocktail (Roche, Germany) and PMSF. Cell debris was removed by centrifugation at 14,000 *g* for 15 min, 4°C. Samples were then precleared by an end-over-end incubation for 1 h, 4°C with Protein A-agarose beads (Pierce) prewashed with lysis buffer. Samples were recovered by pelleting the beads and added into Protein A agarose that had been preincubated overnight (4°C) with monoclonal anti-cMyc (Santa Cruz Biotechnology) antibody and incubated for 4 h, 4°C on a tube rotator. The beads were pelleted by centrifugation (13,000 *g*, 2 s), and the supernatant discarded and washed four times with ice-cold wash buffer [50 mM Tris·HCl, pH 7.4, 300 mM NaCl, 5 mM EDTA, and 0.1% (wt/vol) Triton X-100] and once with ice-cold PBS. The beads were then boiled in 1× SDS sample loading buffer and assayed for presence of immunoprecipitated protein by immunoblotting.

Immunoblotting. IP samples and membrane fractions from the yeast lysate were subjected to SDS-PAGE separation in 10% polyacrylamide gels and transferred onto PVDF membranes (Millipore, Billerica, MA) essentially as described [Sambrook, 2001 #127]. The membranes were blocked in 5% nonfat skim milk, 0.1% Tween-20 in tris-buffered saline (TBS: 150 mM NaCl and 20 mM Tris, pH 7.5) for 1 h. followed by an overnight incubation (at 4°C) with primary anti-NHE8 antibody (WK-69) at 1:2,000 dilution. The secondary antibody, donkey anti-rabbit-horseradish peroxidase (Jackson Immunoresearch Labs) was used at a dilution of 1:5,000. Immunoreactive bands were visualized by enhanced chemiluminescence (GE Healthcare, Buckinghamshire, UK).

Reconstitution of functional proteoliposomes. A modification of the freeze-thaw/sonication methods described in Refs. 23, 44 was used. Briefly, 60 mg/ml of soybean phospholipids type II-S (Sigma) were sonicated to clarity; the lipid suspension was mixed with yeast membrane fractions at a lipid:protein ratio of 10:1 to a final volume of 860 μl in reconstitution buffer containing 20 mM BTP-MES, pH 7.5, 10% glycerol, 25mM $(NH_4)_2SO_4$ and 2.5 mM pyranine. The mixture was sonicated for 4×30 s at 20 W with intermittent pulses using a Branson 450 sonifier, and then rapidly frozen in dry ice and subsequently thawed and resonicated for 3×10 s. The mixture was then loaded into a Sephadex G-50 column (Amersham Biosciences, Buckinghamshire, UK) and the eluate was recovered by centrifugation at 180 *g*. Eluted proteoliposomes were diluted five times in the same buffer and then centrifuged at 100,000 *g* for 30 min. The concentrated proteoliposomes were resuspended in reconstitution buffer and stored at −80°C until used. Control proteoliposomes were prepared similarly, but from AXT3 cells transformed with empty vector. All preparatory steps were conducted at 4°C.

Measurement of buffering capacity. Buffering capacity of proteoliposomes was measured in degassed reconstitution buffer at room temperature (25°C) following a modification of previous methods (7, 47). Briefly, proteoliposomes were diluted 25-fold in reconstitution buffer standardized at pH values 6.5 and 7.5. Known amounts of either NaOH or HCl were added to alkalinize or acidify the suspension. Resting pH values were plotted against buffering capacity. It was assumed that $[CO_2]$ was sufficiently low to reduce the equation $\beta_{total} = \beta_i + \beta_{CO2}$ to $\beta_{total} = dB/dpH = \beta_1$ (where dB is the amount of strong base that would have to be added to the buffer to raise pH by dpH). The mean buffering value used in H^+ flux calculations was derived from buffering capacities at pH 6.6 and 6.8 encompassing the pH range relevant to the initial alkalinization of experimental proteoliposomes after addition of cations.

Measurement of proton efflux in vitro. Change in pyranine fluorescence with pH was measured as the 515-nm emission after excitation at 440 nm using a Pathway HT fluorescence microscope (Atto Bioscience) equipped with a high-resolution Hamamatsu CCD camera. Experimental and control proteoliposomes (25 μl) were acidified following the NH_4^+/NH_3 prepulse technique (47) by addition into NH_4^+-free reconstitution buffer (i.e., 20 mM BTP/MES, pH 7.5, 10% glycerol) in 1 ml chambered Labtek glass slides (Nunc, Rochester, NY) at room temperature (25°C). Fluorescence measurements commenced after allowing the baseline signals to stabilize. Cation/H^+ exchange was initiated by addition of Na^+, K^+, Li^+, and choline chloride salts. Calibration of intravesicular pH against change in pyranine's fluorescence was done using the high potassium/nigericin method (49) equilibration of standardized pH buffers (20 mM BTP/MES, 10% glycerol, 150 mM K^+) set at pH 6.0, 6.5, 6.8, 7.0, 7.2, 7.5, and 8.0. A fluorescence/pH calibration curve was prepared for each data set. Final nigericin concentration was 0.5 μM. To inhibit Na^+/H^+ exchange activity, 50 μM EIPA or 10 μM benzamil-HCl (Sigma) was added into the buffers before addition of proteoliposomes. Exchange activity was stopped by addition of 25 mM $(NH_4)_2SO_4$. To quantify the proton fluxes, the net initial rate, i.e., dpH/dt (for $t = 25$ s), was calculated from the 515-nm emission fluorescence (ΔF_{440}) resulting from addition of chloride cations at 15, 30, 60, 100, and 150 mM concentrations after correcting for the buffering capacity of 20 mM BTP-MES at the starting pH i.e., $J^H = \beta_{total} \times dpH_i/dt$. We did not attempt using BCECF in either the liposomes or the PS120 cell line.

EIPA inhibition assay. PS120 cells expressing *Ae*NHE8::c-Myc were maintained under G418 selection in DMEM media. $^{22}Na^+$ uptake in PS120 cells was done in 12-well format as previously described (40). Briefly, the culture medium was aspirated and wells were washed twice with 1 ml of acid load buffer (50 mM NH_4Cl, 70 mM choline chloride, 1 mM $MgCl_2$, 2 mM $CaCl_2$, 5 mM glucose, 20 mM HEPES-Tris, pH 7.4) and incubated in 1 ml of the same buffer for 30 min at 37°C, 5% CO_2 (32). Cells were then washed in choline chloride buffer (135 mM choline chloride, 1 mM $MgCl_2$, 2 mM $CaCl_2$, 5 mM glucose, 20 mM HEPES-Tris, pH 7.4) and incubated for 5 min at room temperature in 250 μl/well of the same buffer supplemented with 2 mM ouabain and 100 μM bumetanide. To initiate $^{22}Na^+$ uptake, 250 μl of uptake solution (74 kBq/ml of carrier-free $^{22}Na^+$ in choline chloride buffer) were added and cells were incubated for 2 min at room temperature. Uptake solution was also supplemented with 2 mM ouabain and 100 μM bumetanide. To determine *Ae*NHE8's sensitivity to EIPA [5-(*N*-ethyl-*n*-isopropyl)-amiloride], H^+-activated $^{22}Na^+$ uptake was measured in the presence of varying concentrations of EIPA (50 nM to 0.1 mM). Uptake was stopped by adding 1 ml of ice-cold stop solution (135 mM NaCl, 1 mM $MgCl_2$, 2 mM $CaCl_2$, 5 mM glucose, 4 mM KCl, 20 mM HEPES-Tris, pH 7.4). Cells were quickly rinsed four times with the stop solution and then lysed in 0.5 ml of 0.5 N NaOH and neutralized

with an equal volume of 0.5 N HCl. The solubilized lysate was added to 3 ml of scintillation fluid and counted using a Beckman liquid scintillation counter (Fullerton, CA). Background radioactivity levels were determined from control nontransfected cells. Data were normalized to protein concentration as measured using the BCA assay (Pierce). $^{22}Na^+$ uptake values (expressed as % of maximal activity) attributable to the Na^+/H^+ exchanger were calculated as the net $^{22}Na^+$ influx after subtracting background levels in the absence (0 μM) and the presence of 100 μM EIPA. Data (represented as means ± SE) were derived from the average of three experiments each performed in triplicate and analyzed using Origin 6.1 (OriginLab, Northampton, MA).

RESULTS

Sequence of A. aegypti NHE8. A. aegypti NHE8 ORF is encoded by three exons (gene AAEL004485 on Vectorbase: *Aedes aegypti*) covering an 11.61-kb genome sequence (see http://aaegypti.vectorbase.org/?Genome/ExonView/transcript=AAEL004485-RA;db=core). The *Ae*NHE8 protein is 668aa long; it bears close similarity to known NHE8 genes: 78% to *Drosophila* NHE1 (16), 44% to *C. elegans* NHX8 (30), 58% to human, and 58% to mouse NHE8 (18). Transmembrane predictions (http://bp.nuap.nagoya-u.ac.jp/sosui/) indicate that *Ae*NHE8 possesses 12 transmembrane regions that are fairly well conserved among known members of this isoform, whereas the long (165 aa) hydrophilic COOH-terminal domain is divergent across species (Fig. 1).

Expression of AeNHE8 in yeast AXT3 cells. Yeast AXT3 cells lack the Na^+ efflux proteins ENA1–4, the plasma membrane Na^+/H^+ antiporter NHA1, and the prevacuolar antiporter NHX1 making the strain very sensitive to high sodium in growth media (42). These cells therefore serve as a convenient tool when studying Na^+ extrusion and sequestration ability of NHE-like proteins by heterologous protein expression. When *Ae*NHE8 was expressed in AXT3 cells under the control of a GAL 1 promoter, it restored tolerance at up to 100 μg/ml hygromycin B and 70 mM sodium in contrast to control cells transformed with vector alone which failed to grow (Fig. 2, *A* and *B*, and data not shown).

In vitro assay of NHE8's Na^+/H^+ exchange activity in reconstituted phospholipid proteoliposomes. Membranes from the yeast AXT3 strain are ideal for studying Na^+/H^+ exchanger in vitro since background interference by endogenous yeast antiporters is abolished. To determine the transport function of *Ae*NHE8, we reconstituted membrane fractions from yeast cells expressing *Ae*NHE8 and control membranes from yeast cells transformed with vector alone into soybean phospholipids proteoliposomes containing the fluorescent dye pyranine (2.5 mM) and 25 mM ammonium sulfate. The proteoliposomes could be observed under UV light at ×100 magnification. Dilution of both experimental and control proteoliposomes into ammonium-free buffer resulted in internal acidification of the proteoliposomes to a pH of ~6.6 as determined by the diminution of pyranine fluorescence after signal calibration. A plot of variation of fluorescence with pH indicated that change in pyranine fluorescence was linear over the 6.5 to 7.5 range (Fig. 3*A*), and this was subsequently used in calibrating ΔF against ΔpH in the experimental proteoliposomes by linear regression.

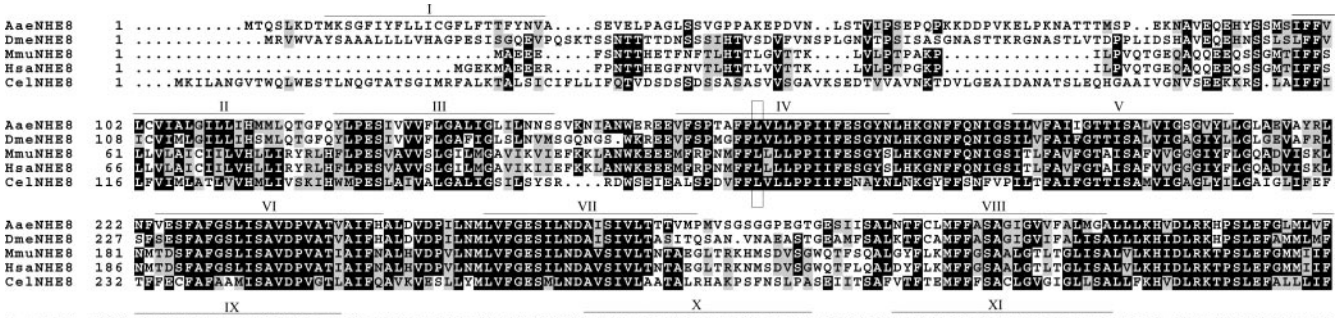

Fig. 1. Sequence alignment and topology of Na^+/H^+ antiporter isoform 8 from *Ae.aegypti*. *A*: alignment of *Ae*NHE8 against a set of known homologs. *Ae*NHE8 like most eukaryotic NHEs has 12 transmembrane domains, and both the NH_2 and COOH termini are predicted to be cytoplasmic. Transmembrane regions are highly conserved, whereas the hydrophilic COOH-terminal region is less well conserved. The transmembrane regions are numbered and marked with bars according to topology prediction generated using SOSUI (http://bp.nuap.nagoya-u.ac.jp/sosui/). The amiloride binding pocket lies in the 4th transmembrane region; the critical leucine (boxed) is replaced with phenylalanine in amiloride-insensitive NHE3. Antibodies used in this study were raised against peptides WK-69 and WK-215; both lie in the hydrophilic COOH terminal. Aae, Dme, Mmu, Has, and Cel refer to *Aedes aegypti*, *Drosophila melanogaster*, *Mus musculus*, *Homo sapiens*, and *C. elegans* (accession numbers AAQ91612, CG12178, Q8R4D1, Q9Y2E8, CAA22320), respectively. *Ae*NHE8 has 53 and 54.2% amino acid identity to human and mouse NHE8 proteins, but this decreases to 38.2 and 41.8%, respectively, when the COOH terminal is considered alone. However, the human and mouse NHE8 COOH termini are 99.1 and 87.6% divergent from that of *Aedes*. The alignment was generated using ClustalX algorithm, whereas the sequence identity and divergence were generated with MegAlign. Residues are shaded along a scale from black through gray to no shade; residues shaded black are completely conserved, and those without any shading are not conserved.

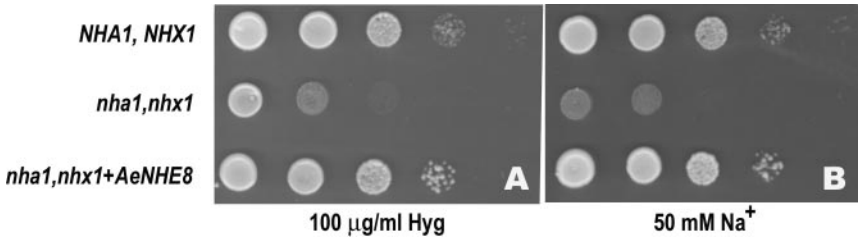

Fig. 2. *Ae*NHE8 complements for *S. cerevisiae NHA1* and *NHX1* functions when heterologously expressed in mutant cells lacking endogenous Na^+ efflux and Na^+/H^+ exchanger proteins. Yeast cells were grown in alkali cation-free AP medium overnight, and cell density was adjusted to an $OD_{600} = 1$. Ten-microliter serial decimal dilutions were spotted on minimal media plates containing 100 μg/ml HygB (*A*) and AP plates containing 50 mM NaCl (*B*). Growth was recorded after 3 days in (*A*) and 4 days in (*B*). G19 strain (*MAT*α, *ade2*, *his3*, *leu2*, *trp1*, *ura3*, Δ*ena1::HIS3::ena4*) was used as *NHA1*, *NHX1*; *nha1*, *nhx1* is the AXT3 strain (*MAT*α, *ade2*, *his3*, *leu2*, *trp1*, *ura3*, Δ*ena1::HIS3::ena4*, *nha1::LEU2*, *nhx1::TRP1*). All expression was under galactose induction and the controls were transformed with an empty vector.

Cation/H^+ exchange was initiated by addition of cations (as chloride salts) at varying concentrations. A 150 mM final cation concentration was used to determine the exchanger's cation selectivity and physiologically relevant rate of exchange. There was negligible increase in fluorescence when cations (up to 300 mM) were added into the control proteoliposomes (Fig. 3*B* and data not shown). Nor was there any increase in fluorescence when ammonium-free buffer was added into the control proteoliposomes. In both experimental and control proteoliposomes, addition of 25 mM $(NH_4)_2SO_4$ restored the internal vesicle pH to ~7.5 as assessed from the resting fluorescence (Fig. 3*B*).

In the experimental proteoliposomes, chloride cations of Na^+, K^+, and Li^+ at concentrations of 15, 30, 60, 100, and 150 mM were used to generate a curve of variation of the rate of exchange (measured as increase in pyranine's fluorescence at 515 nm and assumed to be proportional to rate of H^+ efflux) against cation concentration. The experiments were stopped after ~450 s with the addition of 25 mM $(NH_4)_2SO_4$; alternatively, 0.5 μM nigericin was added to equilibrate the internal and bulk buffer pH. In this case too, the fluorescence was observed to rise sharply. When Na^+ and K^+ ions were added, there was rapid pH elevation while Li^+ had an effect about twofold less efficient. Fluorescence recovery after addition of 150 mM Na^+ attained the equivalent pH of ~7.05. Alkalinization resulting from addition of choline chloride was minimal. We also observed negligible increase in fluorescence in the control proteoliposomes upon addition of 150 mM Na^+ and K^+ which could be attributed to some minor ion leakage (Fig. 3*B* and data not shown). In all cases, the ion exchange reaction exhibited saturable kinetics with increased cation concentration (Figs. 3*B* and 4*A*). Last, dilution of proteoliposomes into buffer containing 25 mM NH_4^+ did not result in any vesicle acidification, and subsequently, addition of cations also had no effect on fluorescence emission.

The kinetic data obtained from the fluorimetric assays were fitted into the Michaelis-Menten equation by the least-squares method. The K_m values were determined as 33 mM for sodium and 41 mM for potassium (Fig. 4*A*). Lithium had a much lower affinity at ~80 mM (data not shown). The maximum rate of alkalinization for sodium was 64 μM/s (which corresponds to 3×10^{-3} ΔpH/s). The three cations Na^+, K^+, and Li^+ all yielded approximate Hill constant values of one ($h = 1$; Fig. 4*B*).

AeNHE8 expression and pharmacological properties in PS120 cells. To explore the expression and pharmacological properties of *Ae*NHE8, we expressed the exchanger in the NHE-deficient PS120 cells. Expression of c-Myc tagged *Ae*NHE8 in stably transfected PS120 cells was confirmed by immunolocalization using both WK-69 and anti-c-Myc antibodies. Both antibodies gave identical results. But unlike human NHE8 which localizes intracellularly in human cell lines (28), *Ae*NHE8 localizes to the plasma membrane and intracellular compartments (Fig. 5, *A* and *B*). To further ascertain the specificity of the antibodies employed in the study, lysates from PS120 cells stably expressing untagged *Ae*NHE8 (control) and c-Myc tagged *Ae*NHE8 were immunoprecipitated (IP) with anti-cMyc monoclonal antibody. The IP samples were immunoblotted with anti-NHE8 polyclonal antibody WK-69. A band running at ~70 kDa was observed (Fig. 6*A*, *lane 2*), that was absent in the control lane (Fig. 6*A*, *lane 1*). In yeast cells, *Ae*NHE8 is expressed as a similarly sized protein, which is also detectable by the anti-NHE8 WK-69 antibody (Fig. 6*B*, *lane 2*). No protein was detected in yeast cells not expressing NHE8.

*Ae*NHE8 contains the conserved sequence for amiloride binding (Fig. 1) likely to render it sensitive to amiloride and its analogs. We first attempted, unsuccessfully however, to establish its sensitivity to both EIPA and benzamil using the in vitro fluorescence assays used above. But from the immunofluorescence results noted above, we found that *Ae*NHE8's expression profile in PS120 cells made these cells amenable for $^{22}Na^+$ uptake assays and for determining the basic pharmacological properties that would compare or distinguish it from other NHEs and Na^+ transporters. The sensitivity of *Ae*NHE8 expressing PS120 cells to amiloride was measured from the inhibitable component of $^{22}Na^+$ uptake in the presence of increasing concentrations of EIPA, from 50 nM to 100 μM. The IC_{50} of *Ae*NHE8 was determined at 1.75 μM from the inhibition curve (Fig. 7). Thus *Ae*NHE8 appears to mediate EIPA-sensitive proton exchange when expressed in exchanger deficient PS120 cells.

Expression of AeNHE8 in mosquitoes. To analyze the tissue distribution of *Ae*NHE8, we raised polyclonal antibodies directed against the COOH terminal using synthetic peptides, WK-215 and WK-69, as antigens (see Fig. 1 for positions of antigen residues). These antibodies were used to examine the expression and distribution of *Ae*NHE8 in adult female and larval tissue sections. As shown in Fig. 8 (probed with anti-

WK-215 antibody), there was intense immunofluorescent signal in the principle cells of Malpighian tubules (Fig. 8, *A* and *C*). *Ae*NHE8 expression was also observed in the rectal pad (Fig. 8, *B* and *E*, ×40) and anterior regions of the hindgut (Fig. 8*B*). However, no expression was detected in the midgut sections (Fig. 8*A*). Under higher magnification, expression in the Malpighian tubules' principal cells was found to clearly localize to the apical membrane, whereas little or no expression was observed on the basolateral membrane or in intracellular structures (Fig. 7*D*). We did not observe NHE8 expression in stellate cells.

Adult and larval tissues were additionally probed with anti-WK-69 antibody and fluorescent signal observed in both the proximal and distal aspects of gastric caecae (Fig. 5*C1* and *C2*) and in the Malpighian tubules of larval and adult female mosquitoes (data not shown since the localization was identical to that obtained above with the anti-WK-215 antibody).

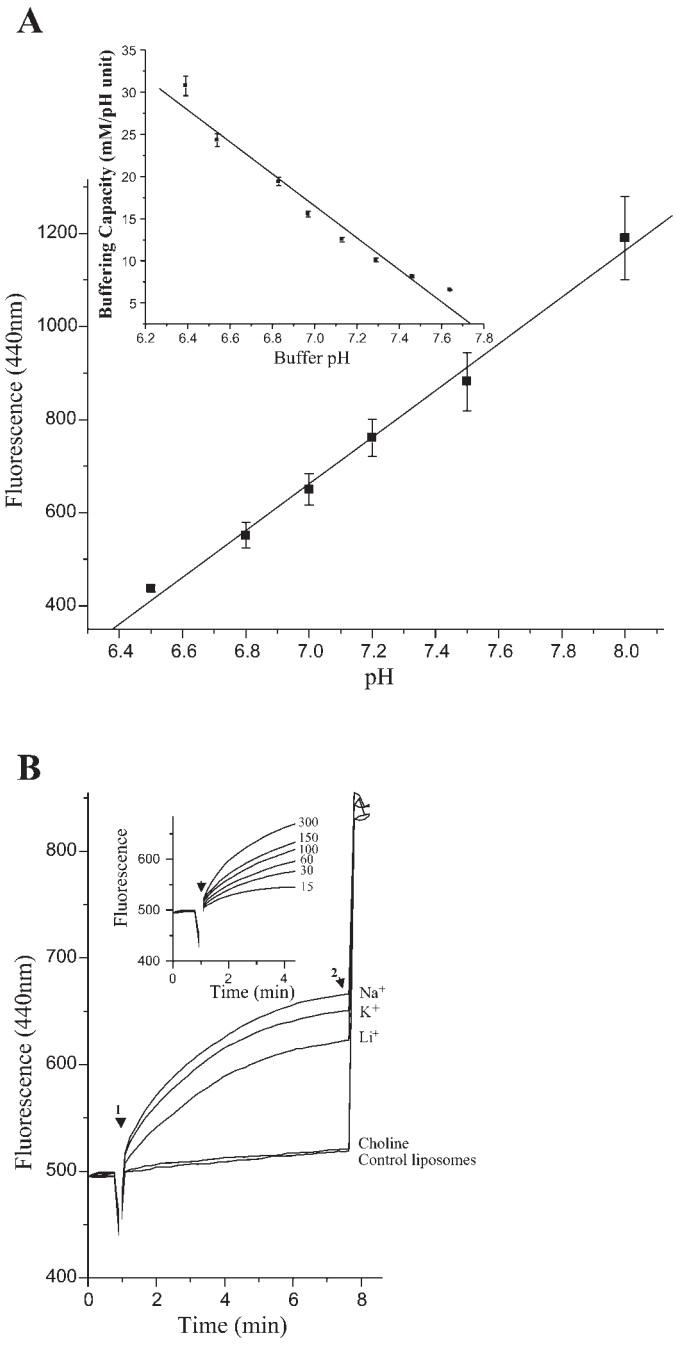

Fig. 3. Cation/H^+ exchange activity in reconstituted phospholipid proteoliposomes. *A*: in vitro calibration curves for pyranine (2.5 mM) fluorescence as a function of pH were prepared at the end of each set of experiments. Proteoliposomes (25 μl) were acidified by addition into 500 μl of NH_4^+-free standardized pH buffers (pH 6.0, 6.5, 6.8, 7.0, 7.2, 7.5, and 8.0); 0.5 μM nigericin was then added to equilibrate intravesicular pH to bulk buffer. pH-sensitive pyranine fluorescence was measured at 440-nm excitation and 515-nm emission. Change in the pyranine fluorescence varies linearly with pH over the 6.5 to 7.5 range. *Inset*: pH dependence of buffering capacity in reconstitution buffer. Data are ± SD ($n = 3$). Total buffering capacity assumes negligible contribution by $HCO_3^-CO_2$, i.e., β_{total} = dB/dpH. *B*: to investigate cation/H^+ exchange activity, 25 μl proteoliposomes from yeast AXT3 cells expressing *Ae*NHE8 (experimental) and from cells transformed with empty vector (control) were acidified (intravesicular) by dilution into 500 μl of NH_4^+-free reconstitution buffer; chloride salts (150 mM) were then added (*arrow 1*) and vesicle alkalinization (measured as increase in fluorescence, 440-nm excitation, 515-nm emission) was recorded. In the control trace, 150 mM Na^+ was added into control proteoliposomes. Rapid increase in fluorescence was observed upon addition of Na^+ and K^+; Li^+'s response was ~2-fold less efficient. Alkalinization resulting from addition of 150 mM choline chloride into experimental proteoliposomes was minimal. Transport activity was stopped by addition of 25 mM $(NH_4)_2SO_4$ which dissipated the H^+ gradient. *Inset*: change of fluorescence (ΔF) increases with cation (Na^+) concentration.

DISCUSSION

In this report, we identified and characterized the mosquito *A. aegypti's* NHE8, a recent addition to the family of Na^+/H^+ exchanger proteins. Our findings here add to previous work done on mammalian NHE8 proteins (17, 18, 28) by providing additional expression and functional data about this isoform. We showed that *Ae*NHE8 is expressed in the apical membrane of the mosquito's Malpighian tubule, gastric caecae, and rectum but not observed in the midgut. We further showed that it retains its Na^+/H^+ exchange function when expressed in the yeast *S. cerevisiae* and in mammalian fibroblast cells. We also described the kinetics and inhibitor sensitivity of its activity in vitro.

In nonblood fed *A. aegypti* mosquitoes, NHE8 is exclusively expressed in the apical membrane of principal cells, which comprise the major cell type in the Malpighian tubules, with no expression in stellate cells. There was also no expression in the midgut. This exclusivity in expression pattern may be an indicator that it has a defined transport function and is not a housekeeping exchanger. Its localization in the plasma membrane of the Malpighian tubules, gastric caecae, and the NHE-deficient PS120 cells distinguish it from human NHE8 expression in Golgi and post-Golgi compartments in human cell lines (28), or the intracellular localization in punctate cytoplasmic structures of NHE8:GFP in transgenic *C. elegans* (30); but it is similar to NHE8 expression in the apical membrane of rat kidney proximal tubules (17, 58). We must note, however, that while it is easy to speculate on *Ae*NHE8 function in the Malpighian tubules, its function in the larval gastric caecae is unclear. There were no obvious differences in *Ae*NHE8 expression between the proximal and distal regions suggesting that the exchanger's function in these poorly characterized resorbing/secreting cells is not spatially differentiated.

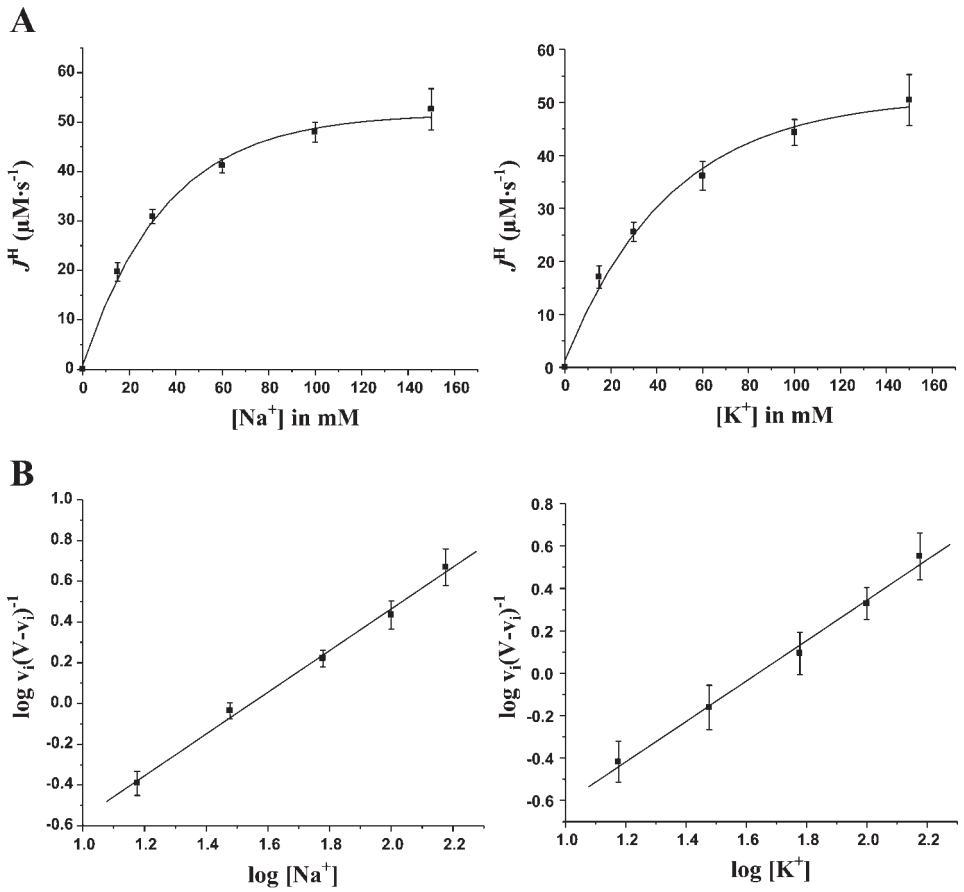

Fig. 4. Kinetics of *Ae*NHE8's exchange activity in reconstituted proteoliposomes. *A*: in vitro Na^+ and K^+/H^+ exchange data obtained were fitted into the Michaelis-Menten equation by least-squares method. Apparent K_m values obtained were 34 mM for sodium (*left*) and 41 mM for potassium (*right*). Lithium had a much lower affinity at 80 mM (data not shown). In the figure, proton flux (J^H) expressed as $\Delta[H^+]/s$ is plotted against external cation concentration. *B*: observed initial velocity of cation/H^+exchange activity and the calculated maximum initial velocity values were used to estimate the Hill constants. Apparent Hill constants for Na^+ and K^+ (0.998 and 0.997, respectively) were linear. Data were from 3 separate experiments.

*Ae*NHE8 runs at ~66 kDa (Fig. 6*B*) when expressed in yeast AXT3 cells. When tagged with a c-Myc epitope and expressed in mammalian lung fibroblast PS120 cells, the protein runs at ~70 kDa which is closer to the estimated size of a 73-kDa protein (Fig. 6*A*). We confirmed the specificity of the antibodies used in this study by immunoprecipitating c-Myc tagged *Ae*NHE8 overexpressed in PS120 cells using antibodies directed at the c-Myc epitope (Fig. 6*A*). The small discrepancy in mass observed in the exchanger expressed in PS120 cells and that in yeast could be a due to the frequently anomalous migration of hydrophobic membrane proteins in SDS-PAGE gels. Another plausible explanation is that the protein undergoes posttranslation modification such as glycosylation given that there are several predicted *N*-glycosylation sites in the exchanger's protein sequence.

The ease of gene manipulation in baker's yeast makes it an attractive model in studying protein function. In this study, we took advantage of yeast cells' sensitivity to high concentration of sodium in the cytoplasm to establish the function of the mosquito exchanger. Sodium tolerance in yeast involves either extrusion through the plasma membrane (45) or sequestration into vacuoles (13). The four plasma membrane Na^+-ATPases (ENA1–4) (13) and the plasma membrane Na^+/H^+ antiporter NHA1 (39) extrude sodium from the cells, whereas the prevacuolar exchanger NHX1 (29) sequesters it in vacuoles. The yeast strain AXT3 has disruptions on all three classes of genes which renders it highly sensitive to high sodium (42). The functionality of NHX1 can also be tested by assaying the yeast cells' tolerance to hygromycin B, although the precise mechanism by which the exchanger imparts this resistance is not yet well understood (15). When expressed in AXT3 cells, *Ae*NHE8 conferred tolerance to a sodium concentration as high as 70 mM (data not shown and Fig. 2). The cells were also able to grow at up to 100 μg/ml hygromycin B indicating that the mosquito exchanger can complement endogenous NHX1 activity. Wild-type yeast cells can grow in media with a maximum sodium concentration of 200 mM (43). Since *Ae*NHE8 is clearly functional in yeast vacuoles, a proportion of the improved tolerance to Na^+ must necessarily be attributable to vacuolar sequestration. In contrast, expression of *Ae*NHE8 in WΔ3 cells (which lack the potassium uptake proteins TRK1 and TRK2) (43) grown in low-K^+ AP media offered no improvement in K^+ uptake (data not shown) confirming, as expected, that the exchanger cannot function as a potassium channel.

Pyranine has previously been shown to be an accurate tool in measuring intravesicular and intracellular pH within the pH range of 6.5 and 7.8 (14, 52) which falls within the physiologically relevant pH range in the mosquito Malpighian tubules (37). Furthermore, yeast membranes have been shown to be efficiently reconstituted into phospholipid proteoliposomes with entrapped pyranine using either the detergent solubilization method (53) or by physical means (23, 44). We used the latter method and confirmed the integrity of the proteoliposomes prepared by achieving sustained intravesicular acidification using the NH_3/NH_4^+ prepulse protocol (47). A 25-fold dilution of ammonium concentration resulted in reduction of intravesicular pH by 0.9 units from 7.5 (pH of the reconstitu-

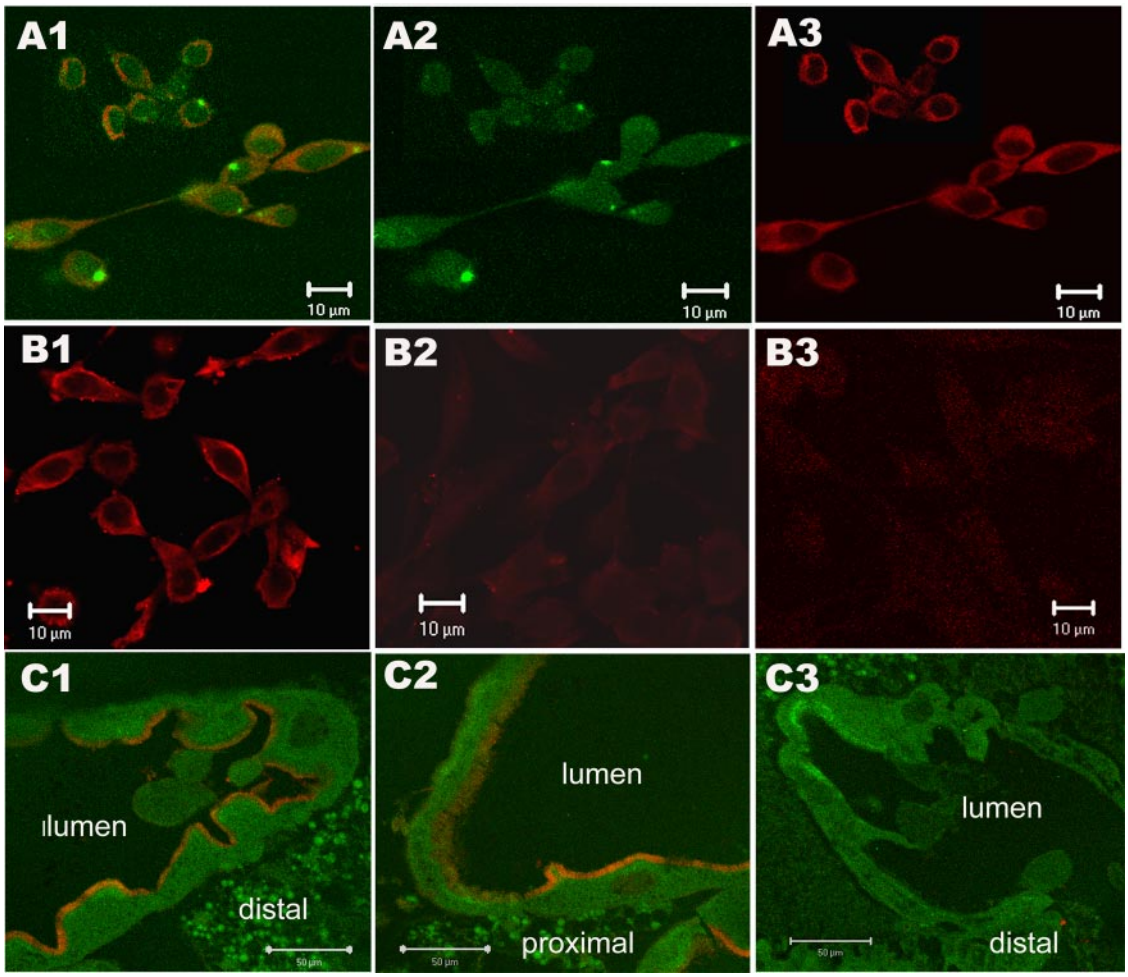

Fig. 5. *Ae*NHE8 expression in PS120 cells and larval gastric caecae. PS120 cells stably transfected with *Ae*NHE8 and paraffin sections of larval tissue were probed for expression of *Ae*NHE8. Cy3-linked secondary antibody (1:1,000) was used to determine exchanger expression, whereas cell and tissue structure were visualized using phalloidin (Alexa-488). *A*: PS120 cells expressing c-Myc tagged *Ae*NHE8 were probed with monoclonal anti-Myc antibody (1:800 dilution). The red channel (A3) shows *Ae*NHE8 expression to be localized to the plasma membrane and intracellular compartments. *A1*: merges Alexa-488 (*A2*) signal with anti-AeNHE8 signal (*A3*). No specific signal was observed in control untransfected cells (*B3*). *Ae*NHE8 signal was also observed in the plasma membrane and intracellularly (B1) using polyclonal anti-NHE8 (WK-69) antibody (1:100 dilution). There was no specific signal in control untransfected cells labeled with the polyclonal antibody (*B2*). *Bottom*: merged Alexa-488 (green) and anti-NHE8 (red) labeling in distal segment of larval gastric caeca (*C1*), proximal gastric caeca (*C2*), and the preimmune control (*C3*). The bright green (*A1* and *A2*) and red (*B1*) spots observed are due to occasional dye precipitation.

tion buffer) to 6.6 (Fig. 3*A*). A similar range was observed in proteoliposomes prepared using the detergent solubilization method (53). When subjected to a steep sodium gradient of 150 mM, the pH recovers halfway to 7.05 in a time period of ~8 min (Fig. 3*A*). The incomplete pH recovery by cation/H^+ exchange may be attributed to the proportion of correctly oriented and functional exchangers in the proteoliposomes: 50% assuming complete randomness in protein orientation with physical proteoliposome reconstitution. Additionally, the nonendogenous nature of the phospholipid environment might not fully recapitulate exchanger function. The fluorescence recovery is, however, full (i.e., to ~pH 7.5) when the bulk external NH_4^+ concentration is raised to match the initial concentration of the reconstitution buffer at 25 mM. A rapid rise in fluorescence was also observed when nigericin was added to the proteoliposomes even after leveling of ΔF following cation addition (data not shown) indicating ion concentrations were still not at equilibrium inside and outside the proteoliposomes. The organic cation choline did not cause any significant fluorescence change (Fig. 3*B*) nor did the addition of cations into control proteoliposomes prepared from membranes of control cells transformed with empty vector. Thus the fluorescence signal (and pH) recovery observed in the experimental proteoliposomes is apparently mediated by *Ae*NHE8.

The in vitro assays using reconstituted proteoliposomes determined that *Ae*NHE8 had a moderately high affinity for Na^+ and K^+ with K_m values of 33 and 41 mM, respectively (Fig. 4*A*), with sodium having a maximum velocity of 3×10^{-3} ΔpH/s. It should be noted, however, that the above cation affinity values are about fourfold less than their physiological concentrations in the mosquito (34), meaning that the exchangers are saturated with the cations at steady state (12). These K_m values are within the range (3–50 mM) reported for other NHEs in different cell types and vesicle preparations (2, 8). Compared with its mosquito homolog, human NHE8 has a much lower affinity at 130 and 75 mM for Na^+ and K^+, respectively, as observed in similar in vitro Na^+ and K^+/H^+ assays (28). The similarity of Na^+ and K^+ affinity values

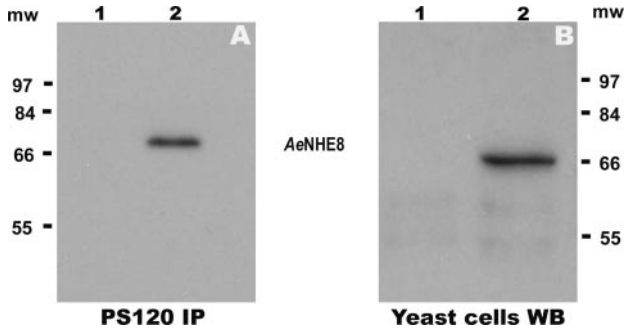

Fig. 6. Immunodetection of *Ae*NHE8 expressed in yeast AXT3 cells and PS120 cells. *A*: IP was done on cell lysates derived from cells stably expressing untagged *Ae*NHE8 (*lane 1*) and c-Myc-tagged *Ae*NHE8 (*lane 2*) using anti-c-Myc monoclonal antibody. Immunoblotting was performed on the immunoprecipitates with the polyclonal anti-NHE8 antibody WK-69. An ~70-kDa band was present in lane loaded with immunoprecipitated c-Myc tagged *Ae*NHE8 that was absent in the control lane. When nontransfected PS120 cells were used instead of cells expressing c-Myc-tagged *Ae*NHE8, no band was observed (data not shown). *B*: results of immunoblotting of yeast membrane fraction using anti-NHE8 WK-69 antibody. The first lane was loaded with membranes from control yeast (transformed with empty vector), whereas the second lane was from cells expressing *Ae*NHE8. The mosquito NHE8 runs at ~66 kDa when expressed in yeast cells. Molecular weight markers are shown on both panels in kDa.

might be interesting when interpreted in the context of post-blood meal diuresis. Although this could simply result from an accommodative cation binding site, the fact that the secretion of K^+ peaks almost an hour (9) after Na^+ raises questions on whether the exchanger contributes to the secretion of both cations.

NHE isoforms have routinely been distinguished by their susceptibility to inhibition by amiloride and its analogs, notably EIPA, which is most potent. The amiloride binding site has been shown to be located within the fourth transmembrane region (8, 12) where a pocket of residues is well conserved among NHEs. This pocket has the sequence "VFFLFLLPPII" and coincides with residues 160–170 in the quintessentially amiloride-sensitive human NHE1 (11). Substitution of the fourth leucine residue with phenylalanine "VFFFFLLPPII" results in insensitivity (11). Furthermore, in the relatively amiloride-insensitive NHE3, the sequence is "VFFFYLLPPII" (8, 40). In *Ae*NHE8, this sequence is "AFFLVLLPPII" (Fig. 1) and we expected it to be sensitive to amiloride based on its sequence fidelity. Besides, the existence of an amiloride-sensitive NHE in the apical membrane of *A. aegypti's* Malpighian tubules has been proposed from electrophysiological studies of whole tubules showing that EIPA disrupts membrane conductance and inhibits salt and fluid secretion (35). We first attempted to understand the sensitivity of *Ae*NHE8-dependent exchange activity to known inhibitors of NHEs using the reconstituted lipid vesicles. EIPA (dissolved in DMSO) was added at concentrations of 5–50 μM to both experimental and control proteoliposomes. A steady increase in fluorescence in both experimental and control proteoliposomes (data not shown) was observed even without addition of cations making the system unsuitable for determining *Ae*NHE8's susceptibility to inhibition by EIPA; similar observations have been previously reported (53). The effect was not caused by DMSO since no change in fluorescence was observed with addition of the solvent alone. Because the anomaly was also observed in vesicles prepared from soybean phospholipids alone, it likely resulted from perturbation of the vesicular lipid bilayer by EIPA. The resultant leakage would then have caused rapid dissipation of the H^+ gradient resulting in fluorescence changes similar to those observed with an increase in pH. Benzamil, another NHE inhibitor, had no significant inhibitory effect on NHE8 activity which was in agreement with findings that it is a poor inhibitor of Na^+/H^+ exchange in the Malpighian tubules of *A. aegypti* (35).

To circumvent this problem, we used the PS120 cell line, an NHE-deficient clone derived from Chinese hamster lung fibroblast cells (38) that has been routinely used in studying pharmacological properties of mammalian NHEs. Based on its expression in Malpighian tubules, *Ae*NHE8 would be expected to function in the forward mode extruding Na^+ from principal cells into the lumen. But NHEs have been known to function in reverse mode under sufficiently strong electrochemical gradient (54). We developed stable PS120 cell lines expressing tagged and untagged *Ae*NHE8 and confirmed the protein's expression in the plasma membrane using both anti-NHE8 and anti-c-Myc epitope antibodies (Figs. 5 and 6). We then subjected the cells to an acid load in Na^+-free buffer and assayed for EIPA-sensitive $^{22}Na^+$ uptake. Confirming our prediction, *Ae*NHE8 showed a dose-dependent sensitivity to EIPA with an IC_{50} of 1.75 μM. Compared with other NHE isoforms, this would rank it as a moderately amiloride-sensitive exchanger (27).

Physiological measurements of transepithelial Na^+ and K^+ concentrations and estimations of H^+ flux mediated by the

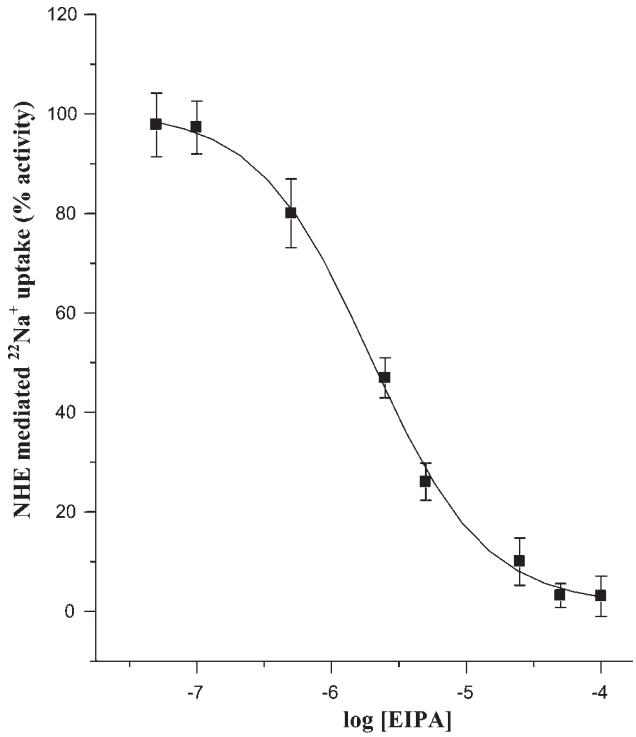

Fig. 7. *Ae*NHE8 sensitivity to EIPA. Inhibition of Na^+/H^+ exchange in PS120 cells stably transfected with *Ae*NHE8, assayed as inhibitable $^{22}Na^+$ influx was measured across a range of EIPA concentrations (50 nM to 0.1 mM) as detailed in EXPERIMENTAL PROCEDURES. Data were normalized as a percentage of the maximal rate of NHE-mediated $^{22}Na^+$ influx in the absence of EIPA. Values (means ± SD) represent the average of 3 separate experiments each done in triplicate.

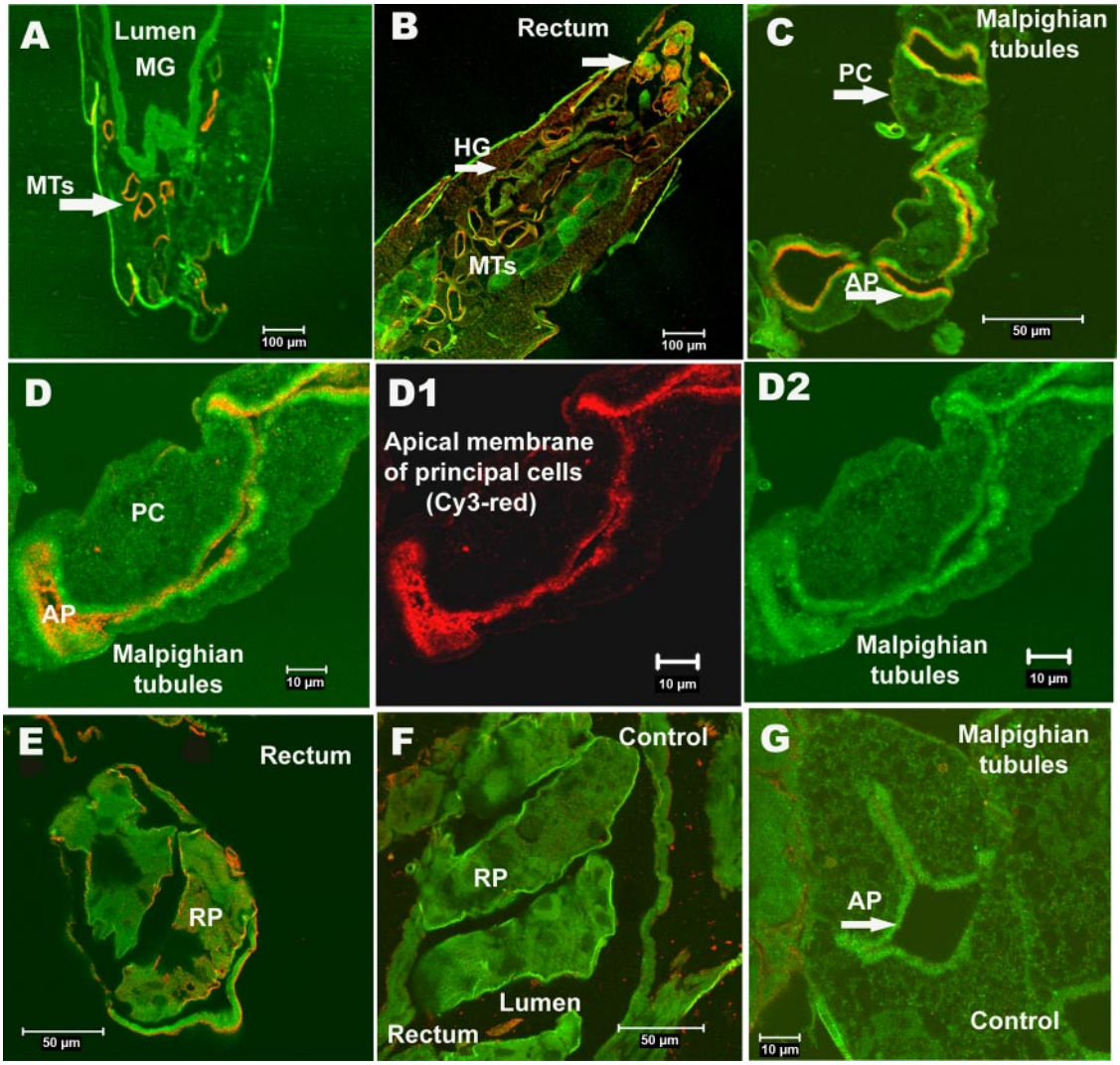

Fig. 8. Tissue and cellular expression of NHE8 in *Ae. aegypti*. Sections of adult female mosquito Malpighian tubule, gut, and rectal tissues showing anti-NHE8 (WK-215) immunoreactivity (red). Phalloidin (green) was used for actin staining. *A*: cross-sectional anti-NHE8Ab reactivity in the apical membrane of Malpighian tubules; no reactivity was observed in the midgut at ×10 magnification. *B*: additional immunoreactivity in the rectum, but none in the anterior hindgut. *C*: higher (×40) magnification of the Malpighian tubules showing reactivity along the apical membrane of the principal cells. *D*: reactivity (×100 magnification) in the apical membrane of the principal cell after merging anti-NHE8 (*D1*) and phalloidin (*D2*) signals. *E*: staining in the rectum (×40 magnification). *F*: rectal and Malpighian tubule sections (*G*) staining controls using the same antibody after preadsorption with antigen. MTs, Malpighian tubules; MG, midgut; HG, hindgut; PC, principal cell; AP, apical membrane; RP, rectal pad.

V-ATPase suggest a cation/H^+ exchange stoichiometry of 1:1 across Malpighian tubule's apical membrane (22, 55). In other Na^+/H^+ exchange activity studies, intracellular and luminal pH appear to be linked to sodium concentration. For instance, removal of extracellular Na^+ also decreases pH_i in the Malpighian tubule cells (35, 37), and inhibition of exchanger activity with EIPA decreases steady-state pH_i in addition to blocking Na^+ and fluid secretion (35). These observations and the pH neutrality of mosquito Malpighian tubules (37) appear to preclude the need for an electrogenic exchanger. Although we could not conclusively settle this question, the calculated Hill constants of 1 for both Na^+ and K^+ (Fig. 4*B*) are consistent with this view. If these observed results are upheld, then *Ae*NHE8's electroneutrality would be in contrast with the $K^+/2H^+$ exchange in lepidopteran gut (25) or the $2Na^+/H^+$ stoichiometry in crustacean NHEs (1).

It is important to note that only five NHEs (isoforms 3, 6, 8, 9, and 10) (41) have been identified in the available dipteran genomes compared with nine in both mammals and *C. elegans* (7). Of those five, the tentatively assigned NHE9 and 10 differ significantly from the rest in sequence and evolutionary relationship while retaining the NHE signature motif (41). Remarkably, there is no apparent equivalent of the mammalian housekeeping isoform NHE1 in dipteran genomes. However, one cannot the exclude the possibility that the five NHE genes in insects can produce multiple splice variants to generate diversity from a smaller number of genes. Indeed, *Ae*NHE3 is expressed as at least two splice variants that differ in their content of regulatory sites (19), thereby raising the possibility of differential targeting and regulation.

Finally, based on this expression and functional data, and also on available electrophysiological data (4, 22, 31, 34, 35),

one might speculate that *Ae*NHE8's activity is coupled to the proton gradient created by the apical V-ATPase to secondarily drive Na^+ or K^+ extrusion across the tubule's epithelia. Future studies should reveal whether this is indeed the case.

ACKNOWLEDGMENTS

We thank Drs. J. M. Pardo and A. Rodriguez-Navvaro for the yeast strains used in this study, Dr. B. L. Barber for sharing PS120 cells, and Dr. D. Carter for assistance with the Pathway HT fluorescence microscope.

GRANTS

W. Kang'ethe was partially supported by the UC Toxic Substances Research & Teaching Program. This project was funded in part by National Institutes of Health Grants AI-32572 and 48049 to S. S. Gill.

Present address of A. K. Pullikuth: Dept. of Pharmacology and Experimental Therapeutics, Louisiana State University Health Sciences Centre, New Orleans, LA 70112.

REFERENCES

1. **Ahearn GA, Mandal PK, Mandal A.** Biology of the $2Na^+/1H^+$ antiporter in invertebrates. *J Exp Zool* 289: 232–244, 2001.
2. **Aronson PS.** Kinetic properties of the plasma membrane Na^+-H^+ exchanger. *Annu Rev Physiol* 47: 545–560, 1985.
3. **Beyenbach KW.** Energizing epithelial transport with the vacuolar H^+-ATPase. *News Physiol Sci* 16: 145–151, 2001.
4. **Beyenbach KW.** Transport mechanisms of diuresis in Malpighian tubules of insects. *J Exp Biol* 206: 3845–3856, 2003.
5. **Beyenbach KW, Pannabecker TL, Nagel W.** Central role of the apical membrane H^+-ATPase in electrogenesis and epithelial transport in Malpighian tubules. *J Exp Biol* 203: 1459–1468, 2000.
6. **Brett CL, Donowitz M, Rao R.** Evolutionary origins of eukaryotic sodium/proton exchangers. *Am J Physiol Cell Physiol* 288: C223–C239, 2005.
7. **Briskin DP, Reynolds-Niesman I.** Determination of H/ATP stoichiometry for the plasma membrane H-ATPase from red beet (*Beta vulgaris L.*) storage tissue. *Plant Physiol* 95: 242–250, 1991.
8. **Burckhardt G, Di Sole F, Helmle-Kolb C.** The Na^+/H^+ exchanger gene family. *J Nephrol* 15, *Suppl* 5: S3–S21, 2002.
9. **Clements AN.** *The Biology of Mosquitoes*. London: Chapman and Hill, 1992.
10. **Coast GMOI, Phillips JE, Schooley DA.** Insect diuretic and antidiuretic hormones. *Adv Insect Physiol* 29: 279–409, 2002.
11. **Counillon L, Franchi A, Pouyssegur J.** A point mutation of the Na^+/H^+ exchanger gene (NHE1) and amplification of the mutated allele confer amiloride resistance upon chronic acidosis. *Proc Natl Acad Sci USA* 90: 4508–4512, 1993.
12. **Counillon L, Pouyssegur J.** The expanding family of eucaryotic Na^+/H^+ exchangers. *J Biol Chem* 275: 1–4, 2000.
13. **Darley CP, van Wuytswinkel OC, van der Woude K, Mager WH, de Boer AH.** *Arabidopsis thaliana* and *Saccharomyces cerevisiae* NHX1 genes encode amiloride sensitive electroneutral Na^+/H^+ exchangers. *Biochem J* 351: 241–249, 2000.
14. **Gan BS, Krump E, Shrode LD, Grinstein S.** Loading pyranine via purinergic receptors or hypotonic stress for measurement of cytosolic pH by imaging. *Am J Physiol Cell Physiol* 275: C1158–C1166, 1998.
15. **Gaxiola RA, Rao R, Sherman A, Grisafi P, Alper SL, Fink GR.** The *Arabidopsis thaliana* proton transporters, AtNhx1 and Avp1, can function in cation detoxification in yeast. *Proc Natl Acad Sci USA* 96: 1480–1485, 1999.
16. **Giannakou ME, Dow JA.** Characterization of the *Drosophila melanogaster* alkali-metal/proton exchanger (NHE) gene family. *J Exp Biol* 204: 3703–3716, 2001.
17. **Goyal S, Mentone S, Aronson PS.** Immunolocalization of NHE8 in rat kidney. *Am J Physiol Renal Physiol* 288: F530–F538, 2005.
18. **Goyal S, Vanden Heuvel G, Aronson PS.** Renal expression of novel Na^+/H^+ exchanger isoform NHE8. *Am J Physiol Renal Physiol* 284: F467–F473, 2003.
19. **Hart SJ, Knezetic JA, Petzel DH.** Cloning and tissue distribution of two Na^+/H^+ exchangers from the Malpighian tubules of *Aedes aegypti*. *Arch Insect Biochem Physiol* 51: 121–135, 2002.
20. **Harvey WR, Wieczorek H.** Animal plasma membrane energization by chemiosmotic H^+ V-ATPases. *J Exp Biol* 200: 203–216, 1997.
21. **Hayashi H, Szaszi K, Grinstein S.** Multiple modes of regulation of Na^+/H^+ exchangers. *Ann NY Acad Sci* 976: 248–258, 2002.
22. **Ianowski JP, O'Donnell MJ.** Electrochemical gradients for Na^+, K^+, Cl^- and H^+ across the apical membrane in Malpighian (renal) tubule cells of *Rhodnius prolixus*. *J Exp Biol* 209: 1964–1975, 2006.
23. **Kasahara M, Hinkle PC.** Reconstitution and purification of the D-glucose transporter from human erythrocytes. *J Biol Chem* 252: 7384–7390, 1977.
24. **Klowden MJ.** *Physiological Systems in Insects*. San Diego, CA: Academic, 2002.
25. **Lepier A, Azuma M, Harvey WR, Wieczorek H.** K^+/H^+ antiport in the tobacco hornworm midgut: the K^+-transporting component of the K^+ pump. *J Exp Biol* 196: 361–373, 1994.
26. **Madrid R, Gomez MJ, Ramos J, Rodriguez-Navarro A.** Ectopic potassium uptake in trk1 trk2 mutants of *Saccharomyces cerevisiae* correlates with a highly hyperpolarized membrane potential. *J Biol Chem* 273: 14838–14844, 1998.
27. **Masereel B, Pochet L, Laeckmann D.** An overview of inhibitors of Na^+/H^+ exchanger. *Eur J Med Chem* 38: 547–554, 2003.
28. **Nakamura N, Tanaka S, Teko Y, Mitsui K, Kanazawa H.** Four Na^+/H^+ exchanger isoforms are distributed to Golgi and post-Golgi compartments and are involved in organelle pH regulation. *J Biol Chem* 280: 1561–1572, 2005.
29. **Nass R, Rao R.** Novel localization of a Na^+/H^+ exchanger in a late endosomal compartment of yeast. Implications for vacuole biogenesis. *J Biol Chem* 273: 21054–21060, 1998.
30. **Nehrke K, Melvin JE.** The NHX family of Na^+-H^+ exchangers in Caenorhabditis elegans. *J Biol Chem* 277: 29036–29044, 2002.
31. **O'Donnell MJ, Ianowski JP, Linton SM, Rheault MR.** Inorganic and organic anion transport by insect renal epithelia. *Biochim Biophys Acta* 1618: 194–206, 2003.
32. **Orlowski J.** Heterologous expression and functional properties of amiloride high affinity (NHE-1) and low affinity (NHE-3) isoforms of the rat Na/H exchanger. *J Biol Chem* 268: 16369–16377, 1993.
33. **Orlowski J, Grinstein S.** Diversity of the mammalian sodium/proton exchanger SLC9 gene family. *Pflügers Arch* 447: 549–565, 2004.
34. **Pannabecker T.** Physiology of the Malpighian tubule. *Annu Rev Entomol* 40: 493–510, 1995.
35. **Petzel DH.** Na^+/H^+ exchange in mosquito Malpighian tubules. *Am J Physiol Regul Integr Comp Physiol* 279: R1996–R2003, 2000.
36. **Petzel DH, Berg MM, Beyenbach KW.** Hormone-controlled cAMP-mediated fluid secretion in yellow fever mosquito. *Am J Physiol Regul Integr Comp Physiol* 253: R701–R711, 1987.
37. **Petzel DH, Pirotte PT, Van Kerkhove E.** Intracellular and luminal pH measurements of Malpighian tubules of the mosquito *Aedes aegypti*: the effects of cAMP. *J Insect Physiol* 45: 973–982, 1999.
38. **Pouyssegur J, Sardet C, Franchi A, L'Allemain G, Paris S.** A specific mutation abolishing Na^+/H^+ antiport activity in hamster fibroblasts precludes growth at neutral and acidic pH. *Proc Natl Acad Sci USA* 81: 4833–4837, 1984.
39. **Prior C, Potier S, Souciet JL, Sychrova H.** Characterization of the NHA1 gene encoding a Na^+/H^+-antiporter of the yeast *Saccharomyces cerevisiae*. *FEBS Lett* 387: 89–93, 1996.
40. **Pullikuth AK, Aimanova K, Kang'ethe W, Sanders HR, Gill SS.** Molecular characterization of sodium/proton exchanger 3 (NHE3) from the yellow fever vector, *Aedes aegypti*. *J Exp Biol* 209: 3529–3544, 2006.
41. **Pullikuth AK, Filippov V, Gill SS.** Phylogeny and cloning of ion transporters in mosquitoes. *J Exp Biol* 206: 3857–3868, 2003.
42. **Quintero FJ, Blatt MR, Pardo JM.** Functional conservation between yeast and plant endosomal Na^+/H^+ antiporters. *FEBS Lett* 471: 224–228, 2000.
43. **Quintero FJ, Ohta M, Shi H, Zhu JK, Pardo JM.** Reconstitution in yeast of the Arabidopsis SOS signaling pathway for Na^+ homeostasis. *Proc Natl Acad Sci USA* 99: 9061–9066, 2002.
44. **Ramirez J, Pena A, Montero-Lomeli M.** H^+-K^+ exchange in reconstituted yeast plasma membrane vesicles. *Biochim Biophys Acta* 1285: 175–182, 1996.
45. **Rodriguez-Navarro A, Quintero FJ, Garciadeblas B.** Na^+-ATPases and Na^+/H^+ antiporters in fungi. *Biochim Biophys Acta* 1187: 203–205, 1994.
46. **Rodriguez-Navarro A, Ramos J.** Dual system for potassium transport in *Saccharomyces cerevisiae*. *J Bacteriol* 159: 940–945, 1984.
47. **Roos A, Boron WF.** Intracellular pH. *Physiol Rev* 61: 296–434, 1981.
48. **Ross LS, Gill SS.** Limited growth PCR screening of a plasmid library. *Biotechniques* 21: 382–384, 386, 1996.

49. **Thomas JA, Buchsbaum RN, Zimniak A, Racker E.** Intracellular pH measurements in Ehrlich ascites tumor cells utilizing spectroscopic probes generated in situ. *Biochemistry* 18: 2210–2218, 1979.
50. **Thompson JD, Gibson TJ, Plewniak F, Jeanmougin F, Higgins DG.** The CLUSTAL_X windows interface: flexible strategies for multiple sequence alignment aided by quality analysis tools. *Nucleic Acids Res* 25: 4876–4882, 1997.
51. **Torrie LS, Radford JC, Southall TD, Kean L, Dinsmore AJ, Davies SA, Dow JA.** Resolution of the insect ouabain paradox. *Proc Natl Acad Sci USA* 101: 13689–13693, 2004.
52. **Venema K, Gibrat R, Grouzis JP, Grignon C.** Quantitative measurement of cationic fluxes, selectivity and membrane potential using liposomes multilabelled with fluorescent probes. *Biochim Biophys Acta* 1146: 87–96, 1993.
53. **Venema K, Quintero FJ, Pardo JM, Donaire JP.** The arabidopsis Na^+/H^+ exchanger AtNHX1 catalyzes low affinity Na^+ and K^+ transport in reconstituted liposomes. *J Biol Chem* 277: 2413–2418, 2002.
54. **Wakabayashi S, Hisamitsu T, Pang T, Shigekawa M.** Kinetic dissection of two distinct proton binding sites in Na^+/H^+ exchangers by measurement of reverse mode reaction. *J Biol Chem* 278: 43580–43585, 2003.
55. **Weng XH, Huss M, Wieczorek H, Beyenbach KW.** The V-type H^+-ATPase in Malpighian tubules of *Aedes aegypti*: localization and activity. *J Exp Biol* 206: 2211–2219, 2003.
56. **Wheelock GD, Petzel DH, Gillett JD, Beyenbach KB, Hagedorn HH.** Evidence for hormonal control of diuresis after a blood meal in the mosquito *Aedes aegypti*. *Arch Insect Biochem Physiol* 7: 75–90, 1988.
57. **Wieczorek H, Brown D, Grinstein S, Ehrenfeld J, Harvey WR.** Animal plasma membrane energization by proton-motive V-ATPases. *Bioessays* 21: 637–648, 1999.
58. **Xu H, Chen R, Ghishan FK.** Subcloning, localization, and expression of the rat intestinal sodium-hydrogen exchanger isoform 8. *Am J Physiol Gastrointest Liver Physiol* 289: G36–G41, 2005.